

IMPLEMENTATION OF INPUT SHAPING ON FLEXIBLE MACHINES WITH INTEGER CONTROLLERS

Gerardo Peláez

William E. Singhose

*Department of Mechanical Engineering
 ETSII University of Vigo
 36200 Vigo.*

*School of Mechanical Engineering,
 Georgia Institute of Technology
 Atlanta, GA 30332USA.*

Abstract: This paper presents an input shaping method for building in real time a shaped velocity profile according to an integer algorithm that determines the command reference signal at each interpolation step. This integer implementation has the drawback of slightly reduce shaping robustness. However, experimental results confirm residual vibration reduction when robust shapers are used in the integer input shaping process. Copyright © 2002 IFAC.

Keywords: Vibration, Input signals, Shaping Filters.

1. INTRODUCTION

Given the increasing use of low-cost controllers to drive mechanical systems in positioning applications and the trend toward faster, lighter, and more flexible structures, control system design and its implementation with such controllers machines is an important topic. Some modern digital servo systems have the structure shown in Fig. 1. They control a motor using an encoder. They consist of an encoder counter, a microcontroller, some form of D/A (Digital-to-Analog) converter, and a power amplifier that delivers current or voltage to the motor. Note that D/A conversion is usually accomplished with a PWM output. For most mechanical systems a 15 KHz or higher PWM frequency is necessary so to that the modulated signal $U(t)$ effectively produces the desired control effort.

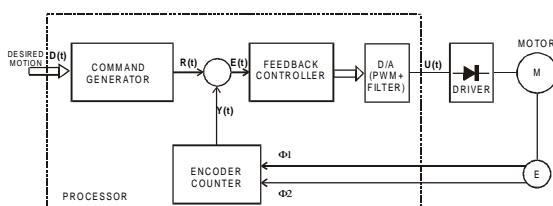


Fig.1. Servo system for motion control.

The command generator is essential for good motion control. A linear piecewise velocity profile is implemented in many of the command generators for position control applications. The velocity profile is trapezoidal when the velocity limit is reached before the midpoint of the motion and triangular for a short move where the velocity limit is not reached.

Input shaping is a technique used in the command generator to reduce residual vibration in mechanical systems with some degree of flexibility. The system parameters (frequency and damping) are used to design the input shaper, which is an impulse sequence whose amplitudes and time location are functions of those parameters. This sequence is convolved with the input and the convolution result is the new shaped input to the system. If the parameters used to design the shaper are accurately known, all or most of the residual vibration would disappear after the time of the last impulse.

A great variety of input shapers has been developed for various types of applications. For example, input shapers have shown benefits for coordinate measuring machines (Singhose et al., 1996) (Jones and Ulsoy, 1999), silicon handling machines

(deRoover and Sperling, 1997), and cranes (Feddemma, 1993) (Lewis et alt 1998) (Singer, Singhose, and Kriikku, 1997). One characteristic that distinguishes each input shaper is its robustness to modeling errors. To evaluate robustness, the residual vibration amplitude is plotted as a function of a modeling error to produce a sensitivity curve. If the vibration increases rapidly with increasing error, then it is not robust. The first input shapers developed in the 1950's suffered from this problem (Tallman and Smith, 1958). These early shapers were designed by requiring zero vibration when the model was perfect, but did not have any requirements to suppress vibration when there were errors in the model.

The zero vibration and derivative (ZVD) shaper was the first input shaper designed to be robust to modeling errors (Singer & Seering 1990). It produces zero vibration when the actual system frequency, ω_a , perfectly matches the modeling frequency, ω_m . Furthermore, the derivative of its sensitivity curve is zero at the modeling frequency. This property of the derivative tends to keep the vibration at a low level, even when there are modeling errors.

Fig. 2 shows a shaped velocity profile for real time motion control. It is the result of convolving the trapezoidal velocity profile described above and a ZVD input shaper. The slope for the convolved profile changes during phases 1 and 2 varying from $A_1 \cdot A$ to A , where A_1, A_2 and A_3 are the ZVD-shaper's impulses amplitudes whose values and application times (ts_2, ts_3) are given in (Singer & Seering 1990). The main goal of this paper is to implement input shaped velocity and position profiles on an integer machine for motion control of mechanical systems with some degree of flexibility.

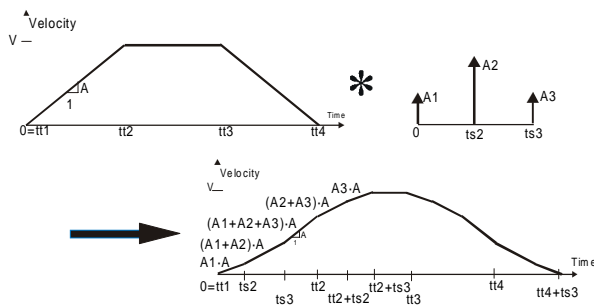


Fig.2. Input shaping a trapezoidal velocity profile.

2. IMPLEMENTING SHAPED CONTROL COMMANDS ON AN INTEGER MACHINE.

As stated in the introduction the driving function is the PWM output given by the microcontroller. Up to 10 bits of PWM resolution is available in most popular microcontrollers, but PWM-frequency and resolution are not independent and must be traded off against each other. As frequency is increased PWM resolution decreases, these are related by:

$$\text{Resolution (Bits)} = \frac{\log\left(\frac{F_{osc}}{F_{pwm}}\right)}{\log(2)} \text{ bits} \quad (1)$$

Where:

FOSC = Clock frequency (4 MHz – 20 MHz).

FPWM = PWM frequency.

From (1), 8 bit resolution with a 4MHz clock is attained for a PWM frequency of around 15 KHz and 10 bits resolution can be achieved with a 20 MHz clock. In addition, a temporized interrupt routine of around one millisecond is necessary to apply impulse amplitudes at the correct times for the shaping process and good motion control. This implies that the modulating $E(t)$ signal can reach up to 1 KHz, so the PWM frequency should not be lower than 15 KHz.

Further development is facilitated if first we restrict the velocity shaped values to increments of the PWM register. To that end, let G be the gain to translate instantaneous velocity values

$$V(k) = V(k-1) + A(k) \quad (2)$$

to the corresponding PWM values.

$$\text{PWM}(k) = \text{PWM}(k-1) + G \cdot A(k) \quad (3)$$

Where:

$V(k)$: Velocity value at k millisecond.

$\text{PWM}(k)$: PWM register value at k millisecond.

$A(k)$: acceleration value at k millisecond.

G : Max PWM value (255) / Max integer velocity value (65535).

This gain G can be easily determined from the maximum value of the PWM signal and maximum value of velocity. Both are integers and equal respectively to $255(2^8)$ and $65535(2^{16})$ for the best resolution due to integer machine constraints as stated above. Note that a unit increment in the PWM value take place at different update time according to

$$\begin{aligned} 1 &= \text{Update_time} \cdot G \cdot A(k) = \\ &= \text{Update_time} \cdot G \cdot A \cdot \sum_{i=1}^k A_i \end{aligned} \quad (4)$$

Where:

Update_time: time between PWM unit increments.

$A(k)$: Acceleration at k millisecond.

A : Nominal acceleration.

A_i : Amplitude of « i » shaper impulse being $i < k$.

Table 1 shows those time values during the acceleration phase for a ZVD shaped velocity profile. The integer discretization process just described above was compared by simulation with a floating point algorithm. Simulations were performed on a mechanical system with low damping $d=0.002$ and natural frequency $\omega_n=3.1416$ [rad· s⁻¹].

Table 1. PWM-Increment time values for a ZVD shaped profile

Acceleration Value	Time interval	Update Time (ms)	PWM Incre.
A1· A	0<t≤ts2	1/G· A1· A	1
(A1+A2=A12) A12· A	ts2<t≤ts3	1/G· A12· A	1
(A1+A2+A3=A123) A123· A	ts3<t≤tt2	1/G· A123· A	1
(A2+A3=A23) A23· A	tt2<t≤tt2+ts2	1/G· A23· A	1
A3· A	tt2+ts2<t≤tt2+ts3	1/G· A123· A	1
0	tt2+ts3<t≤tt3	1	0

Figs. 3 & 4 show residual vibration results for unshaped, ZVD-shaped and ZVD-shaped integer algorithm, velocity profiles. If no modeling errors are assured, it was found that, about 97% of residual vibration reduction can be achieved with the integer algorithm. Note that the shaping increases the rise time of the system, but greatly reduces settling time.

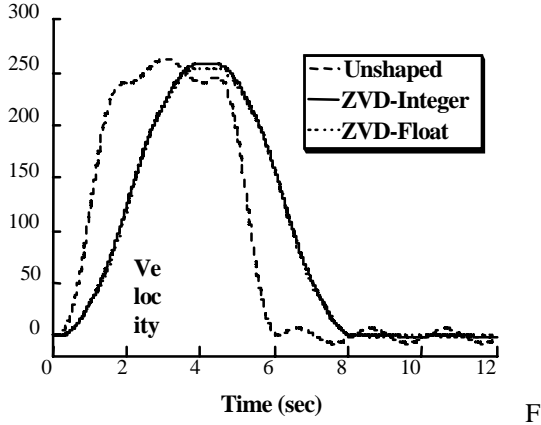


Fig.3. Response to Unshaped, ZVD-integer, and ZVD-float inputs.

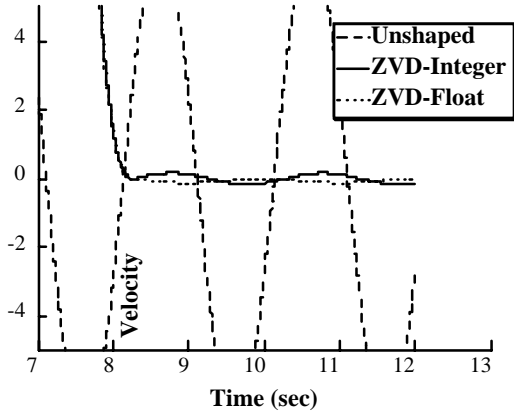


Fig.4. Zoom in on residual vibration from figure 3.

At this point it is necessary to remark that the PWM-output update times given by table 1 must be rounded to the closest millisecond integer value for a standard motion control implementation based on one millisecond temporized interrupt. This rounding process implies a resolution loss that can be estimated by recalculating new acceleration values from the rounded update times according to:

$$I = \text{round}(\text{Update_time}) \cdot G \cdot A'(k) = \text{round}(\text{Update_time}) \cdot G \cdot A \cdot \sum_{i=1}^k A'_i \quad (5)$$

Those slightly modified acceleration values $A'(k)$, implies new amplitudes A_i' for the actual input

shaper implemented that differs from the theoretical values. Fig. 5 shows that those amplitude changes do not cause a significant loss of shaper robustness. To demonstrate this effect the amplitude of residual vibration has been plotted as a function of modeled frequency error. Robustness is usually measured as the width of the curve under some vibration percentage. This non-dimensional parameter I is called the shaper's insensitivity. The results in Fig.5 are only for the set of operating parameters. Other values may lead to lose of robustness when using the integer approximation. To overcome such possible robustness loss some robust shapers are available that in spite of resolution constraints due to integer algorithm approximation can accomplish large insensitivity specifications.

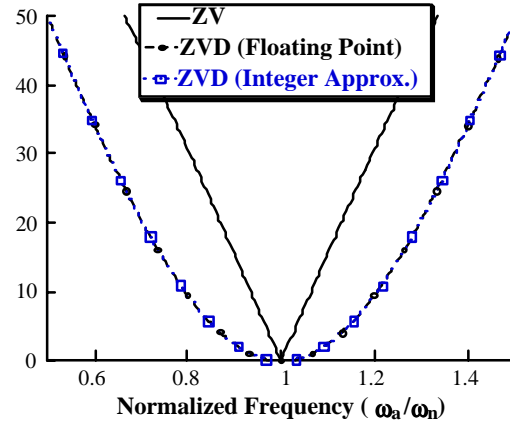


Fig.5. Effect of integer resolution constraints for the ZVD-Shaper.

Specified Insensitive shapers (SI-shaper) can be generated by using a frequency sampling method which consist of repeated use of the expression for residual vibration, in each case the residual vibration is set less or equal to a tolerable level of vibration, V_{tol} (Singer and Seering, 1992) (Singhose et al, 1996):

$$V_{tol} \geq e^{-\delta \omega t_n} \sqrt{(C(\omega, \delta))^2 + (S(\omega, \delta))^2} \quad (6)$$

where C and S are functions of impulses amplitudes, frequency and mechanical system damping. In the following an SI shaper is designed using frequency sampling method with $V_{tol} = 5\%$ and $I = 0.7$. The set of equations that must be satisfied are six versions of (6) at some specified frequencies (see Fig.6). In addition, the impulse amplitudes must sum to one, and have positive values. Solving such a system of non-linear equations with constraints designed for 0.5 Hz modeled frequency and damping $d = 0.002$. The SI shaper is given by:

$$\begin{bmatrix} t_i \\ A_i \end{bmatrix} = \begin{bmatrix} 0 & 0.9767 & 1.9383 & 2.9151 \\ 0.1560 & 0.3440 & 0.3440 & 0.1560 \end{bmatrix} \quad (7)$$

again due to integer implementation according to (5), the SI shaper's amplitudes are slightly modified :

$$\begin{bmatrix} t_i \\ A_i \end{bmatrix} = \begin{bmatrix} 0 & 0.9767 & 1.9383 & 2.9151 \\ 0.1569 & 0.3451 & 0.3346 & 0.1287 \end{bmatrix} \quad (8)$$

The main effect of such differences between theoretical and actual amplitudes is the Shaper's robustness loss as shown in Fig. 6.

In position control mode this analysis remains valid. In this case, the area under the velocity shaped profile curve corresponds to machine position so the command generator approximates the area by performing some kind of numerical integration, Euler's or Tustin methods are available.

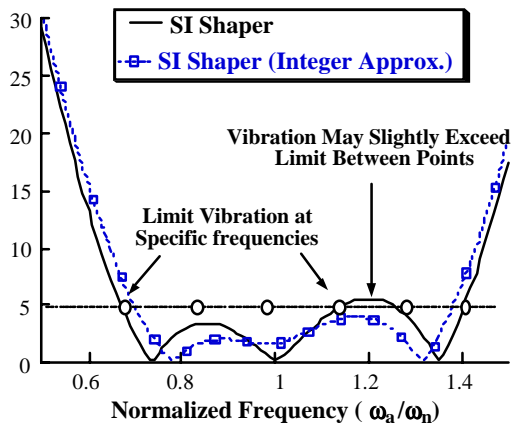


Fig.6. SI-Shaper robustness loss.

In the following analysis the command reference position signal is formulated based on the forward Euler approximation. From Fig. 7, the instantaneous position value $P(k)$ at « k » step can be calculated using a recursive law adding the incremental rectangle area $S(k)$ to the previous position value $P(k-1)$ as shows table 2.

Table 2. PWM-Values at interpolating times.

Interval	Position Value
$0 \leq k < ts_2$	$P(k) = P(k-1) + (k-1) * A_1$
$ts_2 \leq k < ts_3$	$P(k) = P(k-1) + [(ts_2-1) * A_1 + (k-ts_2) * A_{12}]$
$ts_3 \leq k < tt_2$	$P(k) = P(k-1) + [(ts_2-1) * A_1 + (ts_3-ts_2) * A_{12} + (k-ts_3) * A_{123}]$
$tt_2 \leq k < tt_2+ts_2$	$P(k) = P(k-1) + [(ts_2-1) * A_1 + (ts_3-ts_2) * A_{12} + (tt_2-ts_3) * A_{123} + (k-tt_2) * A_{23}]$
$tt_2+ts_2 \leq k < tt_2+ts_3$	$P(k) = P(k-1) + [(ts_2-1) * A_1 + (ts_3-ts_2) * A_{12} + (tt_2-ts_3) * A_{123} + ts_2 * A_{23} + (k-tt_2+ts_2) * A_3]$
$tt_2+ts_3 \leq k < tt_3$	$P(k) = P(k-1) + [(ts_2-1) * A_1 + (ts_3-ts_2) * A_{12} + (tt_2-ts_3) * A_{123} + ts_2 * A_{23} + ts_3 * A_3]$

In addition, the difference between $P(k)$ and $Y(k)$ the actual position given by position sensor, see Fig. 1, is fed into the PWM register. This difference value $S(k)$ is modified to account for the one step delay in the $Y(k)$ signal caused by the control loop. When translating the instantaneous $S(k)$ value to the corresponding PWM value, once again, resolution constraints due to integer approximation arise. Let « G » be the necessary gain for such conversion, that can be estimated from the maximum PWM register value and the maximum incremental rectangle area S_{max} . These are respectively 255 and:

$$S_{max} = (ts_2-1) * A_1 + (ts_3-ts_2) * A_{12} + (tt_2-ts_3) * A_{123} + ts_2 * A_{23} + ts_3 * A_3 \quad (9)$$

then

$$G = \frac{PWM_{max}}{S_{max}} \quad (10)$$

and finally

$$PWM(k) = Round(G * S(k)) \quad (11)$$

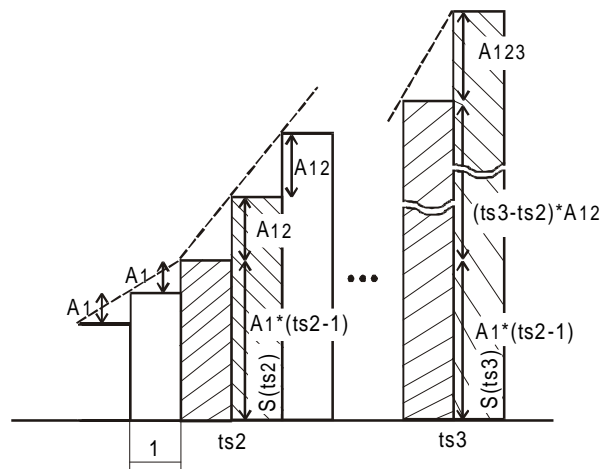


Fig. 7. Numerical integration, forward Euler method.

The effect of numerical approximation, and the PWM resolution constraint just described above was analysed by simulation and compared with an unshaped algorithm. Simulations were performed with the following conditions: mechanical system damping $d=0.002$, natural frequency $\omega_n=3.1$ [rad·s⁻¹], no modeling errors, maximum incremental area S_{max} value 31492, and maximum PWM value 255. Transient deflection and residual vibration reduction with SI-shaper integer approximation was quite effective.

3. DYNAMIC AND EXPERIMENTAL ANALYSIS ON A FLEXIBLE SINGLE INTEGER MACHINE.

Universal joints used in vehicles to transmit power between two shafts that are not collinear need tempering. Some simple machines called picking storage carrousel are used in automated motion sequences needed to feed joints, place them in the working area of a machine tool with a special

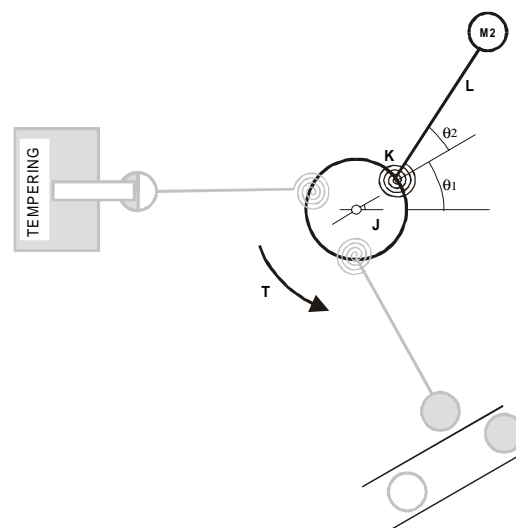


Fig.8. Dynamic model.

tempering headstock and retire the tempered joints. Due to process characteristics, harsh environment conditions are close to the tempering zone so the carrousel shaft and motor must be far from that zone, this implies quite large and flexible arms. A dynamic model for this flexible machine, whose control system is based in a low-cost integer controller, consists of two masses connected by a spring as shown in Fig 9.

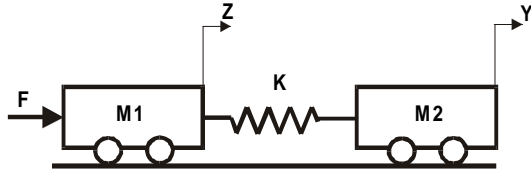


Fig. 9. Benchmark mechanical system.

Applying Newton's second law to this system, we obtain

$$-K \cdot (y - z) = M_2 \cdot \ddot{y} \quad (12)$$

$$F - K \cdot (z - y) = M_1 \cdot \ddot{z} \quad (13)$$

Defining state space variables as follows:

$$x_1 = y; x_2 = \dot{y}; x_3 = z; x_4 = \dot{z}; u = F$$

Then from (12) and (13), we get

$$\dot{x}_2 = -\frac{K}{M_2}(x_1 - x_3) \quad (14)$$

$$\dot{x}_4 = \frac{u}{M_1} - \frac{K}{M_1}(x_3 - x_1) \quad (15)$$

Hence the state space equations are:

$$\begin{bmatrix} \dot{x}_1 \\ \dot{x}_2 \\ \dot{x}_3 \\ \dot{x}_4 \end{bmatrix} = \begin{bmatrix} 0 & 1 & 0 & 0 \\ -\frac{K}{M_2} & 0 & \frac{K}{M_2} & 0 \\ 0 & 0 & 0 & 1 \\ \frac{K}{M_1} & 0 & -\frac{K}{M_1} & 0 \end{bmatrix} \begin{bmatrix} x_1 \\ x_2 \\ x_3 \\ x_4 \end{bmatrix} + \begin{bmatrix} 0 \\ 0 \\ 0 \\ \frac{1}{M_1} \end{bmatrix} u$$

$$y = [1 \ 0 \ 0 \ 0] [x_1 \ x_2 \ x_3 \ x_4]^T \quad (17)$$

Where x_1 and x_3 represent the two angles shown in Fig. 8. The associated eigenvalue problem has the form $\frac{1}{2}I - A \frac{1}{2} = 0$. The solution of this polynomial equation using symbolic computation gives:

$$\lambda_1 = 0; \lambda_2 = 0$$

$$\lambda_3 = \sqrt{\frac{K(M_1 + M_2)}{M_1 M_2}}; \lambda_4 = -\sqrt{\frac{K(M_1 + M_2)}{M_1 M_2}} \quad (18)$$

When the mechanical system shown in Fig. 9 is examined, it is found that, since the masses at each end are not restrained, two rigid-body modes in which both masses move in the same direction by the same amount is possible. The spring is neither stretched nor compressed in those cases. This motion is associated with the zero eigenvalues λ_1, λ_2 and also it is the desirable rigid mode for the motion for the flexible loader system represented in Fig. 8. Thus the frequency of second vibration mode can be

evaluated applying to eigenvalues λ_3, λ_4 the equivalent rotary parameters.

$$\omega_n = \sqrt{\frac{K \cdot (J + M_2 \cdot L^2)}{J \cdot M_2 \cdot L^2}} \quad (19)$$

Note that spring parameter value «K» can be easily estimated from the equivalence of a mass spring system and a balanced beam fixed at its end with the same natural frequency.

$$\sqrt{\frac{K}{M}} = \sqrt{\frac{3 \cdot E \cdot I}{M \cdot L^3}}; K = \frac{3 \cdot E \cdot I}{L^3} \quad (20)$$

By substituting this last equation into (19) we get

$$\omega_n = \sqrt{\frac{3 \cdot E \cdot I \cdot (J + M_2 \cdot L^2)}{J \cdot M_2 \cdot L^5}} \quad (21)$$

Where:

E = Young module.

I = Cross section moment inertia of the uniform arm.

L = Length of the arm.

M2 = Mass at the end.

J = Moment of inertia of the shaft.

An integer command generator for the mechanical system just analysed above was implemented on a PIC16F877 microcontroller. An OMRON absolute encoder EGCP-AG5C-C (resolution 256/360°) was couple to the carrousel shaft with a toroidal joint. Also a board was built to convert the gray code given by the encoder into an analog signal. This sensor was interfaced with our computer, which allow us to write our own virtual instrument to analyse the flexible loader residual vibration. In the first test the mechanical system was moved by the PWM output that feeds a SIEMENS MICROMASTER driver for a standard trapezoidal velocity profile. The size of acceleration and deceleration phases is 3000 ms and the velocity limit is also maintained for the same time length. Residual vibration at the end of the move was measured with our data acquisition system. Fig. 10 shows the sensor signal in the time domain and Fig. 11 in frequency domain.

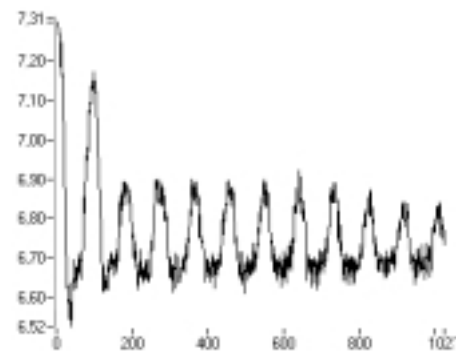


Fig.10. Response of the flexible loader to the unshaped input

Thus from those representations, the measured fundamental frequency of vibration is 0.5 Hz and damping seems to be approximately 0.002. To reduce residual vibration input shaping was used in the integer command generator of this flexible loader.

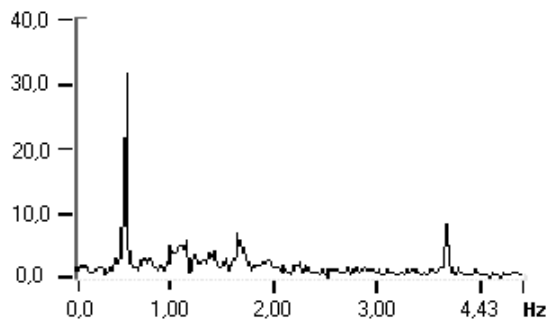


Fig. 11. Frequency components of residual vibration.

The SI-input shaper designed in section 2 for the same mechanical system parameters was implemented by computing the times at which the PWM register must be incremented or decremented according to table 2. Fig. 12 shows the experimental SI-shaped velocity profile generated by the PWM output-port of the PIC.

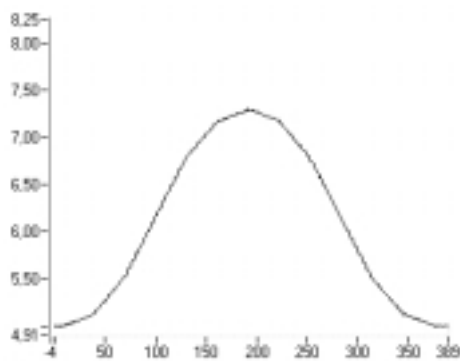


Fig. 12.- Experimental SI-Shaped velocity profile.

The residual vibration of the mechanical system is reduced when the move is generated with this shaped velocity profile as shown in Fig.13. This demonstrates that our implementation of input shaping in a single flexible integer machine can achieve very low residual vibration. As a check the discrete time Fourier transform of this signal is quite similar to the Fourier transform of a square signal that correspond to the fast change of encoder value between 255 and 0 as the loader rotates. As shown in Fig. 14 the amplitude of frequency component

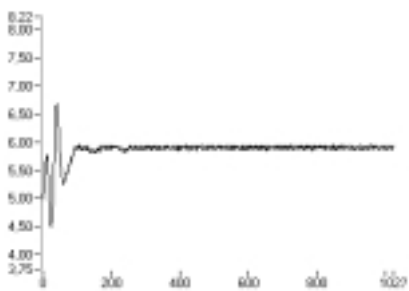


Fig. 13. Residual vibration reduction. corresponding to the flexible loader mechanical vibration at 0.5 Hz is reduced greatly.

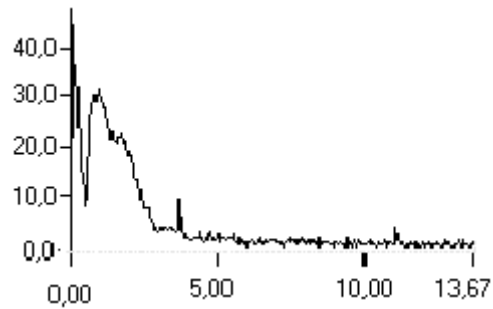


Fig.14. Frequency components of flexible loader sensor signal for SI-shaped input.

4. CONCLUSIONS

An integer implementation of input shaping has been proposed. The method is based on building in real time a shaped velocity profile according to an integer algorithm that determines at each interpolation step the PWM value. The integer approximation reduces the shaper robustness to some degree. However, experimental results confirm significant residual vibration reduction.

REFERENCES

- deRoover D. and Sperling F.B. (1997). Point-Point Control of a High Accuracy Positioning Mechanism. In: American Control Conference Albuquerque, 1997, pp 1350-1354.
- Feddema J.T. (1993). Digital Filter Control of Remotely Operated Flexible Robotic Structures. In: American Control Conf. San Francisco CA, pp 2710-2715.
- Jones S., and Ulsoy A.G., (1999). An Approach to Control Input Shaping Application to Coordinate Measuring Machines. In: Journal of Dynamic Systems, Measurement and Control. pp 242-247.
- Lewis D., Parker G.G., Driessen B., and R.D. Robinet. (1998). Command Shaping Control of Operator-in-the-Loop Boom Crane. In: American Control Conference. Philadelphia, PA.
- Singer, N.C. and Seering, W.P. (1990). Preshaping Command Inputs to Reduce System Vibration. In: Journal of Dynamic Systems, Measurement and Control. March 1990, pp 76-82.
- Singer, N.C. and Seering, W.P. (1992). An Extension of Command Shaping Methods for Controlling Residual Vibration Using Frequency Sampling. In: IEEE International Conference on Robotics and Automation. Nice, France 1992, pp 800-805.
- Singer N., Singhose W., Kriekku E. (1997). An Input Shaping Controller Enabling Cranes to Move Without Sway. In ANS 7th Topical Meeting on Robotics and Remote Systems. Augusta GA.
- Singhose W., Singer N. and Seering W. (1996). Improving Repeatability of Coordinate Measuring Machines with shaped command signals. In Precision Engineering pp 138-146.
- Tallman G.H. and O.J. Smith, "Analog Study of Dead-Beat Posicast Control" IRE Transactions on Automatic Control, March, 1958, pp 14-21.